
VOLUME 51, NOS. 2–3, FEBRUARY 2008
ISSN: 0165-232X
ELSEVIER
cold regions science and technology
SPECIAL ISSUE: INTERNATIONAL SNOW SCIENCE WORKSHOP (ISSW) 2006

Available online at www.sciencedirect.com
ScienceDirect
Cold Regions Science and Technology 51 (2008) 219–228
cold regions science and technology
www.elsevier.com/locate/coldregions

Climate change in western ski areas: Potential changes in the timing of wet avalanches and snow quality for the Aspen ski area in the years 2030 and 2100

Brian Lazar [a,*], Mark Williams [b]

[a] *Stratus Consulting Inc., Boulder, Colorado and American Institute of Avalanche Research and Education, Gunnison, Colorado, USA*
[b] *Department of Geography and Institute of Arctic and Alpine Research, University of Colorado, Boulder, Colorado, USA*

Received 28 September 2006; accepted 30 March 2007

Abstract

We evaluated how climate change resulting from increased greenhouse gas (GHG) emissions may affect the timing of wet avalanches and snow quality at Aspen Mountain in the years 2030 and 2100. Snow quantity was evaluated using the Snowmelt Runoff Model and snow quality was evaluated using SNTHERM. We determined the timing of wet avalanche activity by examining changes to historical average temperatures and snow quality by calculating the bulk density of the top 10 cm of the snowpack. Climate changes were evaluated using MAGICC/SCENGEN and the output from five General Circulation Models (GCMs). The climate change estimates were run using the relatively low, mid-range, and high GHG emissions scenarios: B1, A1B, and A1FI. To get higher resolution estimates of changes in climate, we used output from a regional climate model (RCM, MM5), which is nested in the Parallel Climate Model (PCM).

We defined wet avalanches as likely to occur when average daily temperature exceeds 0 °C and investigated three scenarios: first day when daily average temperature exceeds 0 °C, first three consecutive day period when average temperature exceeds 0 °C, and the day after which average temperature remains greater than 0 °C. By 2030 at the top of Aspen Mountain, wet avalanches are likely to occur between 2 and 19 days earlier than historical averages, with little difference across the GCMs. In 2100, the occurrence of wet avalanches at the top of the mountain varies strongly by CO_2 emissions scenario. The low and mid-range emissions scenarios show that wet avalanches at the top of the mountain start 16 to 27 days earlier than historical averages. In contrast, the high emissions scenario shows wet avalanches occurring 41 to 45 days earlier. In spite of earlier melt initiation and the reduction in snowpack, snow density in the top 10 cm increased by less than 20% by 2030.

Keywords: Climate change; Snow; Avalanche; Ski resorts; General circulation models

Abbreviations: A1B, “middle” GHG emission scenario; A1FI, “high” GHG emission scenario; B1, “low” GHG emission scenario; GHG, Greenhouse Gas; GCM, General Circulation Model; IPCC, International Panel on Climate Change; MAGICC/SCENGEN, Model for the Assessment of Greenhouse-gas Induced Climate Change. SCENGEN stands for Global and Regional Climate SCENario GENerator; PCM, Parallel Climate Model; RCM, Regional Climate Model; SCA, Snow-Covered Area, fraction of total area covered by snow; SNOTEL, SNOpack TELemetry, snow and weather stations maintained by the Natural Resources Conservation Service; SNTHERM, SNow THERmal Model, a 1-D snowpack energy balance model; SRM, Snowmelt Runoff Model, a temperature-index snowpack model; Tmax, maximum temperature; Tmin, minimum temperature.

* Corresponding author. Fax: +1 303 381 8200.
E-mail address: blazar@stratusconsulting.com (B. Lazar).

0165-232X/$ - see front matter © 2007 Elsevier B.V. All rights reserved.
doi:10.1016/j.coldregions.2007.03.015

1. Introduction

Wet snow avalanches are a major safety concern for ski areas in all parts of the world. Although the accuracy of weather and avalanche forecasts is increasing, wet snow conditions continue to pose a difficult hazard management problem for snow safety managers (CAIC, 2005). Spring is a critical season for the Rocky Mountains of North America, when ski areas generate a large percentage of their annual revenue (Gosnell et al., 2006). This period is characterized by increasing air temperatures that cause the snowpack to transition from dry snow to wet snow and transition from dry to wet avalanches. The timing and spatial variability of this transition can be particularly difficult to pinpoint, and the safety concern is further complicated by the difficulty in controlling wet avalanche releases with conventional means such as explosives (Armstrong and Fues, 1976; Romig et al., 2004). Nevertheless, it is important for ski area managers to estimate when snow stability conditions turn from stable to dangerous. Ski area managers use such information to determine when particular ski slopes need to be closed for safety reasons, and to allow them to gauge the financial implications of such closings.

Various forecasting approaches have been used to develop better methods for estimating avalanche hazards (e.g., Bovis, 1977; La Chapelle, 1970; Salaway, 1979; Buser, 1983; Roeger et al., 2001). Wet avalanche release is a complicated phenomenon involving surface energy balance, melt water routing, and liquid precipitation. Despite this complexity, it is widely accepted that air temperature consistently plays a critical role in determining when slopes become susceptible to wet avalanche releases (e.g., McClung and Schaerer, 1993; Roeger et al., 2001; Vojtek, 2002). While studies have investigated the predictive value of weather data for forecasting avalanches (Jamieson et al., 2001; Roeger et al., 2001; Vojtek, 2002), they have focused on short-term (24 h to several days) forecasting horizons.

There is urgency in understanding how the frequency of wet avalanches may change in response to future climate conditions. A fatality at the Arapahoe Basin ski area in May 2005 from a wet avalanche was the first in-bounds fatality in a Colorado ski area since 1976 (CAIC, 2005). One aim of this study is to provide a procedure for estimating spatially and temporally distributed temperature and wet avalanche hazards for future ski seasons using a physically based snow model that can incorporate the output of climate change models. This methodology is designed to be user-friendly and easily transportable to other ski areas. This case study used climate values from five General Circulation Model (GCM) projections for three greenhouse gas (GHG) emissions scenarios to evaluate the likelihood of wet avalanche releases on the Aspen Mountain ski area during the 2030s and 2100s.

We chose the Snowmelt Runoff Model (SRM) (Martinec, 1975; Martinec et al., 1994; model and documentation available at http://hydrolab.arsusda.gov/cgi-bin/srmhome) to determine the presence or absence of snow at various elevations and dates. SRM combines a physically based approach to understanding snow dynamics with climate drivers that are compatible with the output of climate models, particularly air temperature and precipitation. This approach appears to work well in forecasting future snow depths for Aspen Mountain (Lazar et al., 2006). The effect of air temperature on the likelihood of wet avalanches was estimated by focusing on three approaches: the first day when average daily temperature exceeds 0 °C, the first three consecutive day period when average temperature exceeds 0 °C, and the day after which average temperature remains greater than 0 °C.

Our other study objective was to estimate the quality of the snowpack under the climate scenario projected by the Parallel Climate Model/Regional Climate Model (PCM/RCM) climate model. This emissions scenario differs from those used with the GCMs, and assumes a 1% increase in CO_2 concentration per year. We used the Snow Thermal Model (SNTHERM) (Jordan, 1991) to estimate changes in snow density to provide a more detailed analysis of the spatial variability of snowpack characteristics and to address how snow quality could change. Only the PCM/RCM scenario was run because of the need for the full suite of meteorological variables to drive the energy balance model. We analyzed how snow quality differs with different elevations, aspects, and vegetative cover.

2. Study site

Aspen Mountain is located in Pitkin County, Colorado, and lies within the Roaring Fork watershed (Fig. 1). The ski area extends from the 2422 m base area to the 3418 m summit, for a total vertical rise of 996 m. Lack of snow does not currently dictate the end of the ski season. The operational season generally ends in the second week of April because of a decrease in skier visits; snow depth at that time is generally at or near the annual maximum. Several sources of meteorological data exist for the Aspen area and the Roaring Fork watershed that are appropriate for the proposed modeling activities. These include a weather station at the water treatment plant in the City of Aspen (elevation 2484 m), weather stations operated by the ski patrol at the ski area, and a Natural Resources

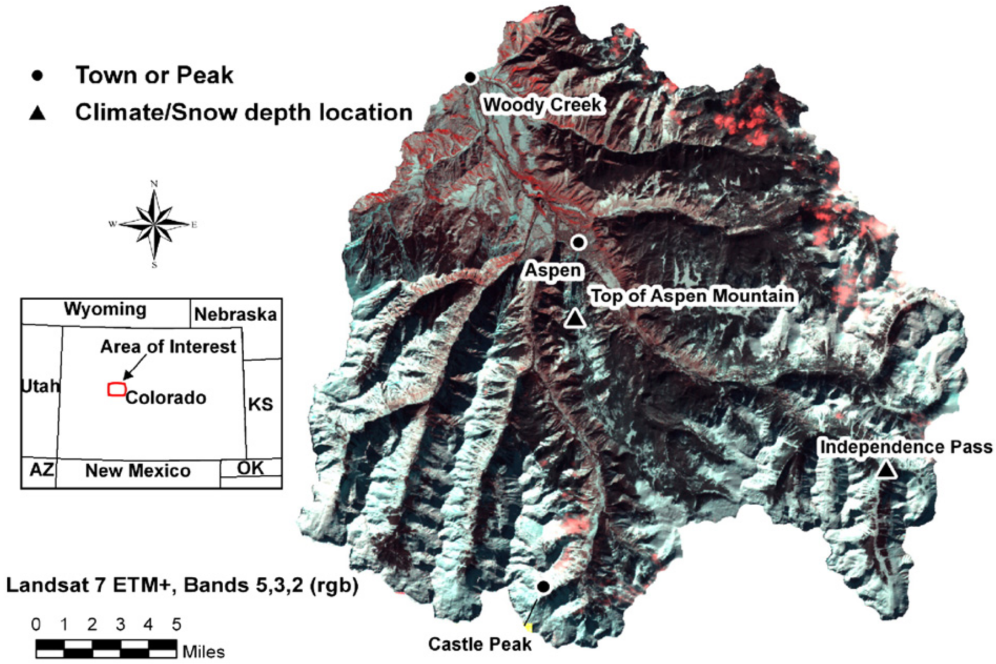

Fig. 1. Location map and modeling domain centered on Aspen Mountain, Colorado, Landsat image.

Conservation Service Snowpack Telemetry (SNOTEL) site located at Independence Pass (elevation 3231 m). Data from the weather station at the top of Aspen Mountain (elevation 3355 m) are available as far back as 1968, but measurements are only made during the winter months when the ski area is operating (mid-November through mid-April). The modeling effort requires full-year datasets, necessitating that we use data from the water treatment plant (2484 m) or Independence Pass (3231 m) since both locations have full-year records. Independence Pass has the closest, most reliable, complete, and representative data available, and was therefore selected as a surrogate for conditions at the upper part of Aspen Mountain. Snow depth during the ski season is measured daily at the top of Aspen Mountain (3355 m) and the mid-mountain station (3059 m), and at the water treatment plant near the base area.

3. Methods

3.1. Climate modeling

We developed scenarios for two time periods: 2030 and 2100. These time periods are not selected to predict weather in a particular future year, but to estimate how average climate conditions may change. The time periods are based on long-term running averages with an approximate 20 year window (Wigley, 2004). The 2030s are within the "foreseeable future" and planning horizons for some industries, and the 2100s capture long-term climate change. Future changes in GHG emissions for these years are difficult to predict and depend on many factors, including population growth, economic growth, technology, government, and society. The Intergovernmental Panel on Climate Change (IPCC) tried to capture a wide range of potential changes in GHG emissions in its Special Report on Emission Scenarios (Nakićenović et al., 2000). The scenarios result in a wide range of emissions and concentrations of GHGs.

Since likelihoods are not given by the IPCC, we used three scenarios from the IPCC that bracket the range of possible emissions scenarios: low (B1), mid-range (A1B), and high (A1FI). Current concentrations of CO_2 in the atmosphere are about 380 ppm. The three scenarios do not diverge much in atmospheric CO_2 concentrations by 2030, so only the mid-range scenario was run for 2030. We bracketed potential climate changes in 2030 using the mean of the five GCMs, a warm–wet model projection (HadCM2), and a warm-dry model projection (ECHAM3). By 2100, the mid-range scenario projects CO_2 concentrations (700 ppm) and temperature warming close to the middle of the range described in the IPCC Third Assessment Report (Houghton et al., 2001). The high-emissions scenario has only slightly higher CO_2 emissions than the mid-range scenario by 2030, but yields 930 ppm CO_2 by 2100. In contrast, the low emissions scenario results in 540 ppm CO_2 by 2100. The high and low emissions scenarios present a stark and interesting contrast between development paths. Based on a recent review by Kerr (2004) of GCM sensitivity to GHG emissions (how much global mean temperature would increase for a doubling of CO_2), we used 3 °C as the central sensitivity estimate.

We used three approaches to evaluate how regional climate will change as GHG concentrations increase. We used the Model for the Assessment of Greenhouse-gas Induced Climate Change and the Global and Regional Climate Scenario Generator (MAGICC/SCENGEN) to understand the regional pattern of relative changes in temperature and precipitation across 17 GCMs (Wigley, 2004). The changes in each GCM are expressed relative to the increase in global mean temperature by the model. This pattern of relative change is preferable to simply averaging regional GCM output because it controls for differences in climate sensitivity across models; otherwise results from models having a high sensitivity would dominate. MAGICC/SCENGEN reports changes in regional climate in 5° by 5° grid boxes. For this study, we used average projections for the grid box where Aspen is located and the adjacent grid box to the north because Aspen is close to the northern edge of its grid box, with the area modeled ranging from 35 to 45°N and 105 to 110°W.

To improve the spatial resolution of changes in climate for the Aspen area, we used two additional approaches. One is the output from the RCM “MM5” (Leung et al., 2003a,b, 2004; Leung and Qian, 2005). RCMs are high-resolution climate models that are built for a region, and are “nested” within a GCM. The RCM MM5 has grid boxes 36 km on a side, about two orders of magnitude less in area than the GCM grids. The model is nested in the PCM (Dai et al., 2004). It is currently not possible to run this model through 2100.

We also used statistical downscaling from GCMs, which assumes that the statistical relationship between the large-scale climate variables in a GCM and a specific location will not change with climate change. The statistical relationship is used to estimate how climate at a specific location may change consistent with the GCM projections for climate change. We used the output from the HadCM3 model (Gordon et al., 1999) and downscaled it to the SNOTEL weather station at Independence Pass. Results did not diverge much from the MAGICC/SCENGEN results and are not reported here but are available from the Aspen Global Climate Change Institute (Katzenberger and Crandall, 2006).

The National Center for Atmospheric Research analyzed how well 17 GCM models simulated current temperature and precipitation patterns for the Earth as a whole and for western North America. The following five GCMs best simulated current temperature and precipitation patterns for western North America and were used in our climate scenarios (Wigley, 2004):

CSIRO — Australia
ECHAM3 — Max Planck Institute for Meteorology, Germany
ECHAM4 — Max Planck Institute for Meteorology, Germany
HadCM2 — Hadley Model, United Kingdom Meteorological Office
HadCM3 — Hadley Model, United Kingdom Meteorological Office.

3.2. Snow modeling

The SRM, developed and maintained by the U.S. Department of Agriculture, Agricultural Research Service (Martinec, 1975; Martinec et al., 1994; model and documentation available at http://hydrolab.arsusda.gov/cgi-bin/srmhome) was used as the primary model to examine potential changes in snow properties for the Aspen area. SNTHERM (Jordan, 1991) was used to provide more detailed information on snow properties and the spatial distribution of those properties about Aspen Mountain.

3.2.1. Snowmelt runoff model

We used the SRM because it is designed to assess snow coverage and snowmelt runoff patterns. The model uses a temperature-index method, which is based on the concept that changes in air temperature provide a surrogate for the overall energy balance of the snowpack. The model runs on a daily time step with drivers that are compatible with GCM outputs: air temperature and precipitation. The modeled domain was 942 km^2, ranging from 2225 m to the 4348 m summit of Castle Peak (Fig. 1). The domain was broken into seven elevation bands of approximately 305 m each.

The SRM accounts for winter precipitation and stores any precipitation event recognized as snow, thereby calculating the maximum snow stored for each elevation band on the defined winter end date. We initiated the model using the model parameters for SRM developed for the nearby Rio Grande River in Colorado (Rango and Martinec, 1999), since that watershed has a similar location, areal extent, and elevation as the Aspen study area. Precipitation was classified as snow when air temperatures were less than 0.75 to 1.5 °C, varying seasonally. Varying the critical air temperature for the formation of snow from 0 to 2 °C did not change the results. Beyond the winter end date, SRM models the melting process and the subsequent depletion of snow-covered area (SCA). We used 2001 as a calibration year for SRM. SCA was estimated approximately once per month using Landsat imagery from 2001. A binary

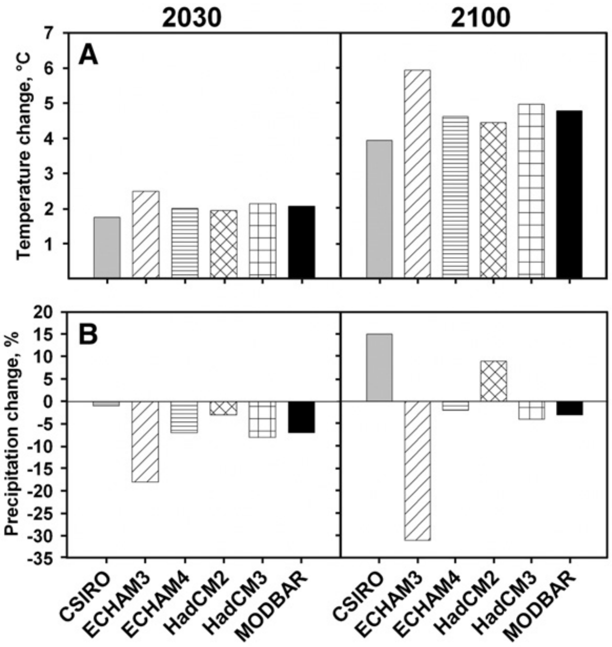

Fig. 2. The projected annual changes in (A) temperature (°C)and (B) precipitation (% change) for the five GCMs for the mid-level (A1B) GHG emissions scenario for the years 2030 and 2100, relative to 1990. The first five bars are results for individual models within MAGICC/SCENGEN; the last bar (MODBAR) is average of the five models.

classification scheme was used to classify each 30-m pixel as either snow-covered or nonsnow-covered (Klein et al., 1998; Dozier and Painter, 2004). Linear interpolation between estimated SCA values from Landsat generated the required daily SCA time series.

3.2.2. SNTHERM

SNTHERM is a process driven, one-dimensional energy and mass balance point model. The snowpack is subdivided vertically into layers; the number of layers and the depth of each layer are set by the user. Using meteorological variables at an hourly time step, the model simulates snow density, grain size, snow depth, and snow temperature for each layer within the snowpack. For this study, we developed 12 landscape types that have relatively homogeneous snow properties from a combination of elevation, aspect, and vegetative cover. Elevation was classified as low (2134 to 3048 m), medium (3048 to 3659 m), or high (3658 to 4267 m). Aspect was defined to be either northerly or southerly, and vegetative cover was either with trees or without trees. We modeled the same spatial domain used in the SRM. Since SNTHERM model results apply only to the conditions at a point, landscape types were used to extrapolate point results spatially, by accounting for energy balance differences unique to each landscape type (Anderson, 2005).

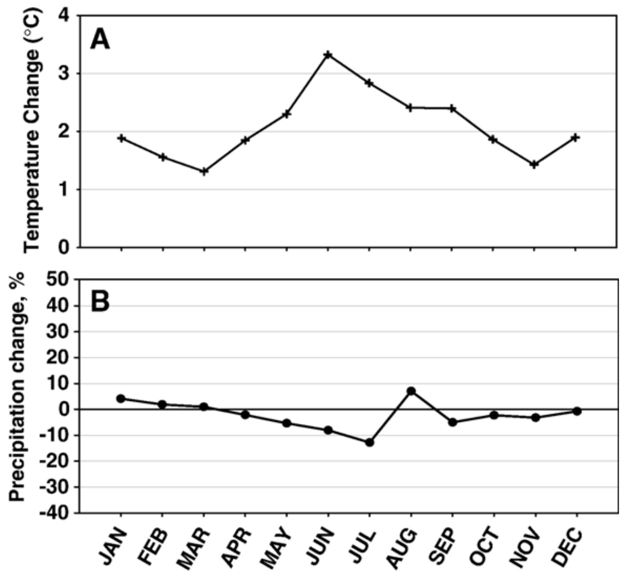

Fig. 3. GCM model average monthly changes in (A) temperature (°C) and (B) precipitation (% change) for the mid-level (A1B) GHG emissions scenario in 2030, relative to 1990.

We modeled snowpack properties for both current (1980–2000) and future (2020–2040) climate scenarios generated by the downscaled PCM/RCM to assess the potential impacts of global climate change on snowpack characteristics. Only the PCM/RCM scenario generates the full suite of meteorological variables required to drive the energy balance model. We estimated snow quality for each landscape type by calculating the bulk density of snow that people ski on, the top 10 cm of the snowpack.

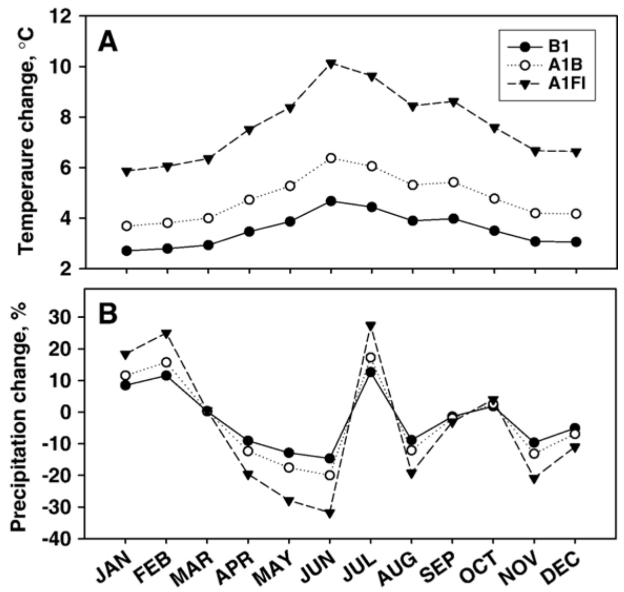

Fig. 4. GCM model average monthly changes in (A) temperature (°C) and (B) precipitation (% change) by GHG emission scenario for 2100, relative to 1990.

4. Results and discussion

4.1. Climate change scenarios

Fig. 2A presents estimated changes in air temperature for Aspen in 2030 and 2100 (relative to 1990) using the mid-range emissions scenario. Under this scenario, the average model warming is 2 °C with a range of 1.8 to 2.5 °C by 2030. By 2100, the average annual temperature increases by 4.8 °C with a range of 4 to 6 °C. Fig. 2B presents the estimated changes in precipitation for the same mid-range emissions scenario. All five models estimate a decrease in annual precipitation for Aspen by 2030. The decreases range from 1% to 18% and average 7%. The average decrease in precipitation by 2100, 3%, is smaller, but the range is greater. The wettest of the five models estimates a 15% increase in annual precipitation, while the driest estimates a 31% decrease. Thus, in contrast to modeled air temperature, there is much more variance among the GCMs for precipitation changes. This pattern of warming throughout the 21st century, along with variable precipitation patterns, is consistent with climate projections for mountain areas in Europe (Beniston, 2006), Australia (Hennessy et al., 2003), and Canada (Scott et al., 2003).

Fig. 3A displays the average monthly changes in temperature for the mid-range emissions scenario in 2030, and Fig. 3B illustrates changes in precipitation. There is little difference among the three emissions scenarios in 2030 because there is little divergence in atmospheric concentrations of CO_2. Therefore, only projections for the mid-range emissions scenario for 2030 are presented here. Fig. 4 displays the average monthly temperature and precipitation changes for the low, mid-range, and high scenarios in 2100. For both 2030 and 2100, air temperature increases occur primarily in the summer months, with summer temperature increases about 50% greater than winter month increases. All scenarios show an increase in monthly precipitation during January and February, followed by strong declines in precipitation during April, May, and June.

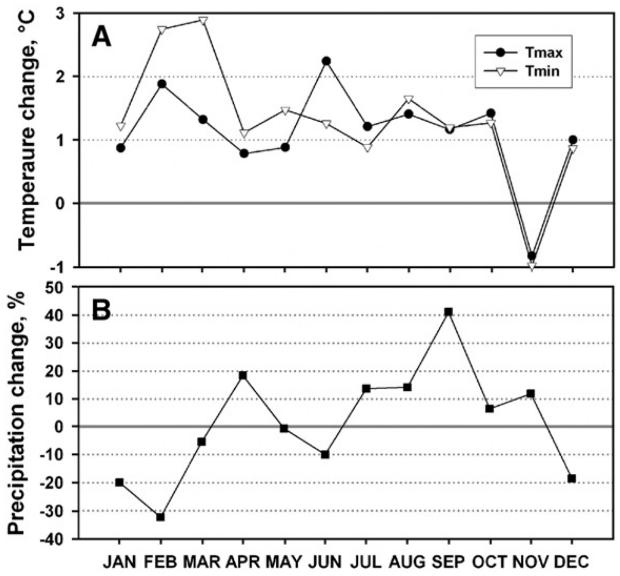

Fig. 5. Estimated monthly changes in (A) temperature (°C) and (B) precipitation (% change) from PCM/RCM for 2030 relative to 1990 for the Aspen grid box. Changes are reported as 2030 minus 1990.

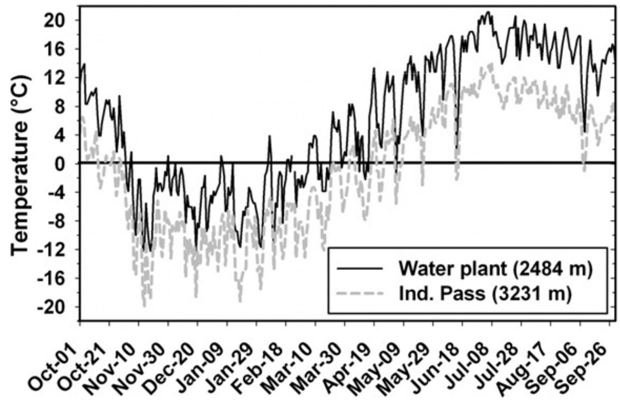

Fig. 6. Average daily air temperature (°C) in 2001 measured at the Aspen water treatment plant and the SNOTEL site at Independence Pass, Colorado.

Fig. 5A displays PCM/RCM estimated increases in maximum temperature (Tmax) and minimum temperature (Tmin), and Fig. 5B shows change in precipitation. The figures compare average projections of temperature and precipitation in 2030 (averaging model simulations for 2020 to 2040) compared to the base period in the RCM of 1990 (1980–2000). The RCM projects an increase in temperature for each month except November, which is difficult to explain (Ruby Leung, Pacific Northwest Laboratory, personal communication, November 17, 2005). On average, total annual precipitation is projected to remain about the same, although the RCM projects a decrease in precipitation from December through March, and an increase in April and again during late summer and early fall. The regional model results are quite different from the GCM results, particularly in seasonality. The RCM projects the largest temperature increases in February and March, whereas the MAGICC/SCENGEN set of GCMs project the largest temperature increases in June and July. Furthermore, the RCM projects decreased precipitation in December through March, while many of the GCMs project increases in January and February.

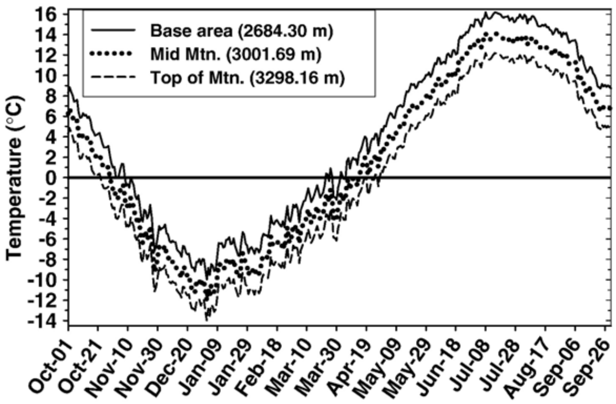

Fig. 7. Historical average (1968–2005) daily average temperatures (°C) for the base area, mid-mountain, and top of the mountain on Aspen Mountain. The expressed values are the hypsometric mean elevations (in meters) of each elevation zone.

4.2. SRM model development

Daily mean air temperature for 2001 was distributed over the seven elevation bands using a lapse rate developed between the climate station located at the City of Aspen and the SNOTEL site at Independence Pass. There was a significant relationship between daily air temperature measured at the City of Aspen and at the Independence Pass SNOTEL site ($y=1.06\times+6.86$, $R^2=0.97$, $n=365$, $p<<0.001$) (Fig. 6). The resulting lapse rate was 0.65 °C/100 m. Average daily air temperatures for both locations drop below 0 °C in the second week of November, and rise above 0 °C by the end of April. At Independence Pass, mid-winter air temperatures decreased to near −20 °C.

Next, a relationship between snowfall amounts for Independence Pass and Aspen Mountain was determined to estimate snowfall amounts at Aspen Mountain during the non-operating season when the ski patrol was not active. The relationship was developed by comparing cumulative snow water equivalent between the two sites for days when both sites were operational.

Snowfall was highly correlated between the two sites, with an R^2 of 0.98 ($y=1.06\times+1.28$, $n=169$, $p<<0.001$). We scaled daily measurements of snowfall from Independence Pass to Aspen Mountain using this regression equation.

SRM was used to determine whether or not snow was present to avalanche during the time periods when defined critical temperature conditions were achieved.

4.3. Timing of wet avalanches

To qualitatively assess potential changes in the occurrence of wet avalanches, we imposed the projected changes in future air temperatures (Figs. 2–4) on the historical average temperatures (1968–2005) (Fig. 7) for each elevation zone on Aspen Mountain. Fig. 8 illustrates the results of the three defined approaches used to quantify the likelihood of temperature-induced wet avalanche releases for the top of Aspen Mountain. By 2030 at the top of Aspen Mountain, wet avalanches are likely to occur between two and 19 days earlier than historical averages, with little difference across the GCMs. The wet climate projection suggests wet avalanches occurring two to 12 days earlier, while the dry climate projection suggests wet avalanches occurring 12

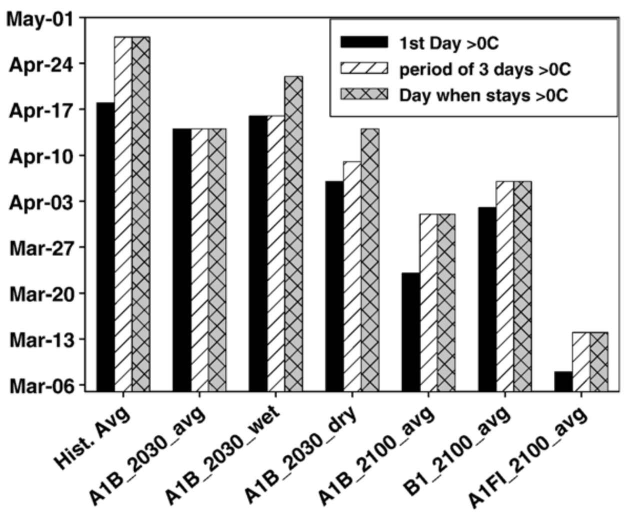

Fig. 8. The dates at which wet avalanche releases become likely at the top of Aspen Mountain, as determined by three defined temperature scenarios.

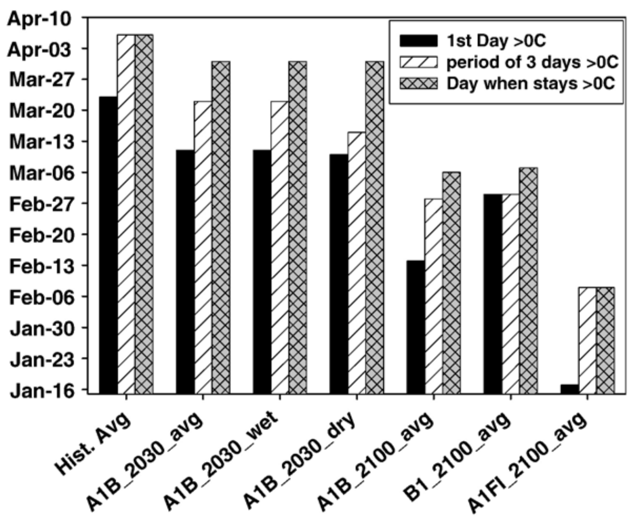

Fig. 9. The dates at which wet avalanche releases become likely at the base area of Aspen Mountain, as determined by three defined temperature scenarios.

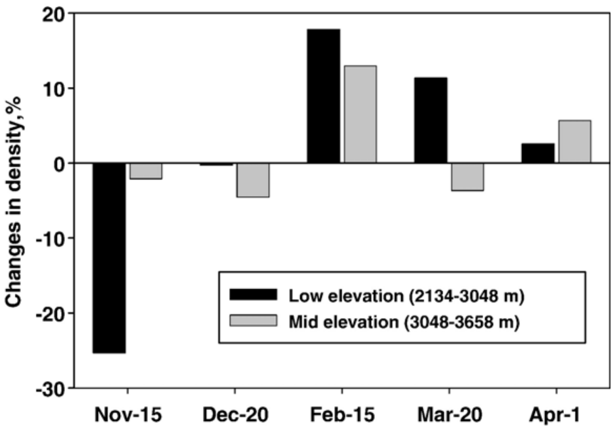

Fig. 10. Changes in the bulk density of the top 10 cm of the snowpack by elevation by 2030, relative to 1990. Dates are approximate for a typical snow season by 2030.

to 19 days earlier. The wet avalanche approach that is defined as the first three consecutive day period when daily average air temperature exceeds 0 °C projects the largest departure from historical average dates of wet avalanche occurrence. This same pattern is evident at the base area, with wet avalanches generally likely to occur six to 22 days earlier by 2030, and little variance among GCMs (Fig. 9). Similar to the top of the mountain results, the approach defined as the first three consecutive day period when average temperature exceeds 0 °C projects the largest departure from historical average dates, with the dry climate projection scenario suggesting the largest shift in timing.

In 2100, the change in the occurrence of wet avalanches at the top of the mountain varies strongly by CO_2 emissions scenario. The mid-range emissions scenario shows that wet avalanches at the top of the mountain start 25 to 27 days earlier than historical averages, while the low emissions scenario projects a shift to 16 to 22 days earlier. In contrast, the high emissions scenario shows wet avalanches occurring 41 to 45 days earlier. By 2100, wet avalanches at the base area are likely to occur 22 to 36 days earlier for the low emissions scenario, 31 to 37 days earlier for the mid-range scenario, and 57 to 65 days earlier for the high emissions scenario.

4.4. Snow quality

New snow density in the top 10 cm of snow at Aspen Mountain during mid-winter currently ranges from about 50–120 kg/m^3 during new snow conditions to 200–250 kg/m^3 several days after the most recent snowfall. In general, lower elevations show an increased density of approximately 3% to 18% from mid-winter to early March (Fig. 10). The mid-elevations are not as affected, but still show a substantial increase in density for February. There was very little difference in snow quality between northerly and southerly aspects, although the increased February density is still apparent. The decrease in estimated density in November is the result of the regional model's estimate of a decrease in November air temperatures. The lack of significant variation in snow density by aspect during mid-winter conditions is driven by cold air temperatures and low sun angle. We interpreted the small percentage increase in future snow density that is superimposed on the current low densities to indicate that Aspen will continue to have relatively low-density new snow. A projected increase in density of 20% raises the average density of new snow at Aspen Mountain to about 90 kg/m3. For 2030, the modeling results suggest that Aspen will retain its low-density new snow characteristic of a cold, high-elevation, continental climate.

5. Conclusions

Wet avalanche hazards will continue to be a concern for ski area operations throughout the remainder of the 21st century, regardless of the emissions scenario. Despite the projected increases in air temperature, snow cover will still persist, on at least some portions of the ski area, well into the spring skiing season. The extent of spring snow coverage on Aspen Mountain varies with emissions scenario. The entire ski area is likely to be snow-covered under the low emissions scenario, while only the top third will retain spring snow under the high emissions scenario. In the future, the initiation of wet avalanches will occur during the operational ski season. Ski area managers may be forced to close certain portions of their available terrain before snow coverage would otherwise dictate, which could have substantial economic impacts for ski areas that rely heavily on spring skiing revenue. More research on predicting and controlling wet avalanches may be warranted.

Snow density is projected to increase by less than 20% in the top 10 cm of the snowpack by 2030, which in our judgment, does not substantially reduce the quality of the snow. By 2100, densities could be substantially higher as a result of warmer temperatures. In spite of increasing snow density, Aspen is likely to retain its characteristic continental climate powder snow through 2030.

Acknowledgements

This research was funded and supported by Stratus Consulting Inc., the Aspen Global Climate Change

Institute, the City of Aspen, and the American Institute of Avalanche Research and Education. Additional support was supplied by the National Science Foundation through the Niwot Ridge LTER program.

We thank Russ Jones of Straus Consulting Inc. for his GIS analysis, Joel Smith of Stratus Consulting Inc. for his comments on climate modeling, and Craig Anderson for his snow modeling support. We also thank Diane Callow and Erin Miles of Stratus Consulting Inc. for their help with document formatting and review.

We appreciate the helpful comments from two anonymous reviewers and from Kate LeJeune who proofread a draft of this manuscript.

References

Anderson, C.R., 2005. Modeling spatially-distributed snowpack properties to enhance our understanding of snow-elk relationships in the Northern Elk Winter Range, Yellowstone National Park. Masters Thesis, University of Colorado-Boulder, CO.

Armstrong, R.L., Fues, J.D., 1976. Avalanche release and snow characteristics. Inst. Arctic Alpine Res., Occas. Pap. 19, 67–81.

Beniston, M., 2006. Mountain weather and climate: a general overview and a focus on climatic change in the Alps. Hydrobiologia 562, 3–16.

Bovis, M.J., 1977. Statistical forecasting of snow avalanches, San Juan Mountains, Southern Colorado, U.S.A. J. Glaciol. 18, 87–99.

Buser, O., 1983. Avalanche forecast with the method of nearest neighbors: an interactive approach. Cold Regions Science and Technology, 8. Elsevier Science Publishers B.V., Amsterdam, pp. 155–163.

CAIC, 2005. Arapahoe Basin May 20, 2005. Available at: http://geosurvey.state.co.us/avalanche/Default.aspx?tabid = 44#AB05202005. Accessed 7/24/2006.

Dai, A., Washington, W.M., Meehl, G.A., Bettge, T.W., Strand, W.G., 2004. The ACPI climate change simulations. Clim. Change 62 (1–3), 29–43.

Dozier, J., Painter, T., 2004. Multispectral and hyperspectral remote sensing of Alpine snow properties. Annu. Rev. Earth Planet. Sci. 32, 465–494.

Gordon, C., Cooper, C., Senior, C., Banks, H., Gregory, J.M., Johns, T.C., Mitchell, J.F.B., Wood, R., 1999. Simulation of SST, sea ice extents and ocean heat transports in a coupled model without flux adjustments. Clim. Dyn. 16, 147–168.

Gosnell, H., Travis, W., Preston, G., 2006. Socioeconomic impacts and adaptation. In: Katzenberger, J., Crandall, K. (Eds.), Climate Change and Aspen: An Assessment of Impacts and Potential Responses. Aspen Global Change Institute, Aspen, CO, pp. 57–80.

Hennessy, K., Whetton, P., Smith, I., Bathols, J., Hutchinson, M., Sharples, J., 2003. The Impact of Climate Change on Snow Conditions in Mainland Australia. CSIRO Atmospheric Research, Aspendale, Victoria, Australia.

Houghton, J.T., Ding, Y., Griggs, D.J., Noguer, M., van der Linden, P.J., Xiaosu, D., Maskell, K. (Eds.), 2001. Climate Change 2001: The Scientific Basis. Cambridge University Press, New York.

Jamieson, B., Geldsetzer, T., Stethem, C., 2001. Forecasting for deep slab avalanches. Cold Reg. Sci. Technol. 33 (2–3), 275–290.

Jordan, R., 1991. A one-dimensional temperature model for a snowcover: technical documentation for SNTHERM.89. Special Report 657. US Army Cold Regions Research and Engineering Laboratory, Hanover, NH.

Katzenberger, J., Crandall, K. (Eds.), 2006. Climate Change and Aspen: An Assessment of Impacts and Potential Responses. Aspen Global Change Institute, Aspen, CO. Available at http://www.agci.org/aspenStudy.html.

Kerr, R.A., 2004. Three degrees of consensus. Science 305, 932–934.

Klein, A.G., Hall, D.K., Siedel, K., 1998. Algorithm intercomparison for accuracy assessment of the MODIS snow — mapping algorithm. Proceedings of the 55th Annual Eastern Snow Conference, Jackson, New Hampshire, June 2–3, 1998, pp. 37–45. Available at http://geog.tamu.edu/klein/publications/proceedings/esc_1998.pdf.

La Chapelle, E.R., 1970. Principles of avalanche forecasting. Ice Engineering and Avalanche Forecasting and Control. Technical Memorandum No. 98. National Research Council of Canada, Associate Committee on Geotechnical Research, pp. 106–113.

Lazar, B., Smith, J., Williams, M., 2006. Estimating changes in climate and snow quantity at the Aspen ski area for the years 2030 and 2100. Proceedings of the 74th Western Snow Conference, Las Cruces, New Mexico, April 17–20.

Leung, L.R., Qian, Y., 2005. Hydrologic response to climate variability, climate change, and climate extreme in the U.S.: climate model evaluation and projections. In: Wagener, T., Franks, S., Gupta, H.V., Bøgh, E., Bastidas, L., Nobre, C., Galvão, C.O. (Eds.), Regional Hydrological Impacts of Climatic Change — Impact Assessment and Decision Making. IAHS Pub., vol. 295, pp. 37–44.

Leung, L.R., Qian, Y., Bian, X., 2003a. Hydroclimate of the western United States based on observations and regional climate simulation of 1981–2000. Part I: seasonal statistics. J. Climate 16 (12), 1892–1911.

Leung, L.R., Qian, Y., Bian, X., Hunt, A., 2003b. Hydroclimate of the western United States based on observations and regional climate simulation of 1981–2000. Part II: mesoscale ENSO anomalies. J. Climate 16 (12), 1912–1928.

Leung, L.R., Qian, Y., Bian, X., Washington, W.M., Han, J., Roads, J.O., 2004. Mid-century ensemble regional climate change scenarios for the western United States. Clim. Change 62 (1–3), 75–113.

Martinec, J., 1975. Snowmelt-runoff model for stream flow forecasts. Nord. Hydrol. 6 (3), 145–154.

Martinec, J., Rango, A., Roberts, R., 1994. The Snowmelt Runoff Model (SRM) User's Manual. In: Baumgartner, M.F. (Ed.), Geographica Bernensia. Department of Geography, University of Berne, Switzerland.

McClung, D.M., Schaerer, P., 1993. The Avalanche Handbook. The Mountaineers, Seattle, WA.

Nakićenović, N., Alcamo, J., Davis, G., de Vries, B., Fenhann, J., Gaffin, S., Gregory, K., Grubler, A., Jung, T.Y., Kram, T., La Rovere, E.L., Michaelis, L., Mori, S., Morita, T., Pepper, W., Pitcher, H., Price, L., Raihi, K., Roehrl, A., Rogner, H., Sankovski, A., Schlesinger, M., Shukla, P., Smith, S., Swart, R., van Rooijen, S., Victor, N., Dadi, Z., 2000. Emissions Scenarios. A Special Report of Working Group III of the Intergovernmental Panel on Climate Change. Cambridge University Press, Cambridge, UK.

Rango, A., Martinec, J., 1999. Modeling snow cover and runoff response to global warming for varying hydrological years. World Resour. Rev. 11 (1), 76–91.

Roeger, C., McClung, D., Stull, R., Hacker, J., Modzelewski, H., 2001. A verification of numerical weather forecasts for avalanche prediction. Cold Reg. Sci. Technol. 33, 189–205.

Romig, J.M., Custer, S.G., Birkeland, K., Locke, W.W., 2004. March wet avalanche prediction at Bridger Bowl ski area, Montana. Proc. Int. Snow Sci. Workshop, Jackson Hole, WY. October.

Salaway, A.A., 1979. Time-series modeling of avalanche activity from meteorological data. J. Glaciol. 22 (88), 513–528.

Scott, D., McBoyle, G., Mills, B., 2003. Climate change and the skiing industry in southern Ontario (Canada): exploring the importance of snowmaking as a technical adaptation. Clim. Res. 23, 171–181.

Vojtek, M., 2002. Meteorological conditions and avalanche formation in the High Tatra Mountains. Meteorol. J. 5 (4), 1–7.

Wigley, T.M.L., 2004. MAGICC/SCENGEN. National Center for Atmospheric Research, Boulder, CO. Available at http://www.cgd.ucar.edu/cas/wigley/magicc/. Accessed June 2005.